Sebastian Bąba[1], Grzegorz Palesa[1], Jarosław Wiśniewski[1], Filip Mańka[1]

Research and Development Department, TRUMPF Huettinger Sp. z o.o., Zielonka 05-200, Poland (1)

doi:10.15199/48.2024.05.06

Considerations on SiC MOSFET TSEP-based junction temperature measurement routines in practical use

Abstract. *Despite being discussed in multiple papers, practical implementation of TSEP-based junction temperature measurement method for SiC MOSFETs causes significant challenges, especially when used in real-life power converters. Challenges which are not usually considered in conference nor journal pares are related to applicability, repeatability and accuracy, especially in comparison to other well-established techniques. To fill this gap in the state of the art, various test routines for junction temperature estimation based on SiC MOSFET on-state channel resistance measurement were compared.*

Streszczenie. *Pomimo omawiania tematu pomiaru temperatury złącza tranzystorów SiC MOSFET w oparciu o ich parametry elektryczne w wielu artykułach, pomiar ten dalej nastręcza wielu trudności - w szczególności przy wykorzystaniu w rzeczywistych przekształtnikach energoelektronicznych. Wyzwania, które z reguły są pomijane w artykułach badawczych dotyczą wykonywalności, powtarzalności i dokładności pomiaru, w szczególności przy porównianiu do innych dobrze znanych metod pomiaru. Aby wypełnić tę lukę, porównano różne sposoby estymacji temperatury złącza w oparciu o pomiar rezystancji kanału tranzystora SiC MOSFET.* ***(Praktyczne wykorzystanie metod pomiaru temperatury złącza tranzystora SiC MOSFET w oparciu o parametry elektryczne)***

Keywords: SiC, MOSFET, TSEP, junction temperature
Słowa kluczowe: SiC, MOSFET, TSEP, temperatura złącza

Introduction

Various degradation mechanisms in power semiconductor devices are accelerated by temperature, which makes junction temperature measurement an essential step in power converter reliability assessment. Although it sounds like a relatively simple task, practical realization of such measurement brings many technical challenges, which made it a very interesting research topic. Unfortunately, both conference and journal papers in this field of study tend to neglect the issues of applicability, repeatability and accuracy of such measurement. A study on SiC MOSFET junction temperature measurement, which could be easily introduced into daily operation of R&D laboratory focusing on power converter design was therefore initiated. The goal was to establish a procedure which 1) is easy to conduct, 2) does not require the use of highly specialized equipment, 3) is immune to environmental conditions, 4) can be performed without significant interference with the tested circuit, and offers satisfactory accuracy ($\pm 5°C$).

This paper is organized as follows: the overview of junction temperature measurement techniques includes a discussion aimed at finding the most suitable approach for standard test routine. A characterization of several Thermosensitive Electrical Parameters (TSEPs) for SiC MOSFET is then presented. Next, two junction temperature measurement routines are proposed, and leading factors on measurement accuracy for those routines are presented. Conclusions are given at the end of this paper.

State of the Art

As presented in Tab. 1, junction measurement techniques can be divided into two main groups: those which require direct contact with the semiconductor chip and those which do not require such access. Although the first group of techniques offers great accuracy, their applicability is limited to specially prepared modules (e.g. without silicon gel) or decapsulated devices [1], which can rarely be used in real-life power converters due to limited reliability and immunity to environmental factors. An example of such a specimen is presented in Fig. 1 where an IR camera was used for direct, contactless junction temperature measurement. Besides customized power module, this figure provides a good depiction of the second limitation of direct measurement techniques – the design of a real-life power converter is optimized to keep it as packed as possible, therefore there is rarely enough space around the power semiconductor device to get access to it with a thermal camera and/or contact thermal probes. Measurement of the electroluminescence effect faces the same limitations.

Table 1. Overview of Junction Temperature Measurement Techniques

Direct	Contact	Thermocouple
		Thermistor [2]
		Optic fiber temperature probes [3, 4]
		Silicon-based sensors
		Liquid Crystal-based sensors
	Contactless	Infrared Measurement [1]
		Electroluminescence Effect [5]
Indirect	Thermosensitive Electrical Parameter (TSEP)	Threshold Voltage [6]
		On-state Channel Resistance [7]
		Breakdown Voltage
		Body Diode Forward Voltage Drop [8]
		Gate Voltage Plateau [9]
		Turn-on/Turn-off delay [10]
		Turn-on transient (di/dt) [11]
		Internal Gate Resistance [12]
	Based on the Case temperature [13]	
	Based on the reference temperature [14]	

Besides direct access to the semiconductor chip, and the space required to set up logging equipment, the next challenge related to the use of contact thermal probes is insulation. The semiconductor chip usually blocks hazardous voltage which could damage data logger or cause harm or death to the operator performing the measurement. Thus, either the probe tip touching the semiconductor chip has to be sealed and insulated (as in the case of a thermocouple or thermistor), or the measurement signal has to be transferred through a transreceiver providing reinforced isolation (as in the case of a silicon-based sensor), or the whole sensor has to be made of non-conducting material (as in the case of optic-fiber temperature probes).

Some manufacturers of power semiconductor devices offers modules with an inbuilt temperature sensor, but unfortunately this is not standard for transfer-mold packages (e.g. TO-247, SOT-227B), which are utilized extensively in power electronics. Also, such a temperature sensor is usually put onto Direct-Bonded Copper (DBC) instead of a semiconductor chip. Such a sensor therefore does not really measure junction temperature, but rather something in between heatsink and chip temperature.

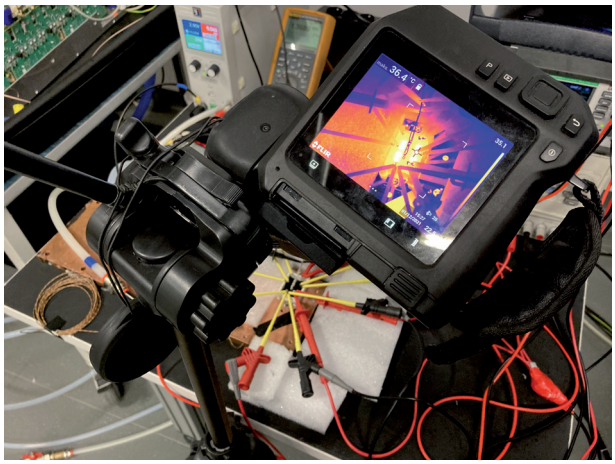

Fig. 1. Infrared junction temperature measurement of customized power module - assembled without lid, nor silicon gel, and covered with dedicated black coating. Laboratory voltage sources and meters were used to control and measure amount of dissipated power.

An alternate approach is the indirect junction temperature measurement, which can be based on a recording of some reference temperature or some electrical parameter which changes proportionally to the junction temperature, also called Thermosensitive Electrical Parameters (TSEPs). A special case of this first method is when the reference temperature is measured just beneath the casing of the semiconductor device, and the power loss dissipated in the semiconductor chip is known. The junction temperature can then be estimated by Eq. 1:

$$T_J = P_{LOSS} \cdot R_{TH_{JC}} + T_C \tag{1}$$

where, T_J is junction temperature, P_{LOSS} is dissipated power, $R_{TH_{JC}}$ is thermal impedance junction-to-case, and T_C is case temperature. This method is very popular due to its simplicity, however it has several flaws which heavily impact measurement accuracy. The main disadvantage is the necessity of P_{LOSS} estimation, which is very challenging for high frequency and/or rectangular-shape signals [15, 16]. Another source of measurement error is the simplification behind thermal impedance. In a real semiconductor device, heat spreads non-uniformly, in accordance with the thermal conductivity of a particular layer (e.g. die attach, copper heatspread), forming isotherm lines. Thermal impedance junction-to-case is defined for the shortest route between heat source and external surface of baseplate, and therefore the accuracy of junction temperature measurement is dependent on *where* the reference temperature is recorded. This phenomenon is particularly easy to spot in the case of SiC devices, where chips are significantly smaller than in Si devices, resulting in a smaller radius of isotherm lines (see Fig. 2).

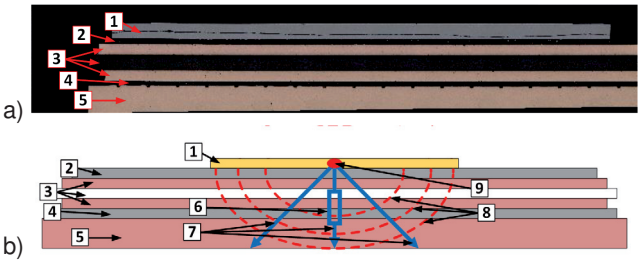

Fig. 2. Microscopic a) and schematic b) cross-section of power semiconductor device. 1) semiconductor chip, 2) die attach, 3) DBC, 4) solder, 5) baseplate (heatspread), 6) thermal impedance junction-to-case, 7) temperature drop vectors, 8) isotherm, 9) heat source.

Another concept relying on reference temperature measurement is presented in [14], where junction temperature is estimated based on the housing temperature (T_{TOP}) instead of case temperature (T_C). Such an approach allows an increase in the range of monitored temperatures from $+5°C...+10°C$ above heatsink temperature, to $80°C...120°C$. This approach is also very simple to use, but is very inaccurate if following assumptions are not met:

1. Amount of losses dissipated in the semiconductor device is known.
2. Environmental conditions are the same during T_J measurement and during the thermal characterization routine.

These assumptions are essential, as resin does not conduct heat very well. Thus, although semiconductor housing heats up proportionally to the junction temperature, it is not a proportional relationship which could be modeled with thermal impedance, and it heavily depends on multiple environmental factors, e.g. ambient temperature, air flow around the device or dissipated power. A graphical representation of the $T_{TOP} \sim T_J$ relationship, and actual difference between them for various levels of power losses, are given in Fig. 3. The final disadvantage, common for both this method and that previously described, is the rather long response time, which makes these methods insufficient for temperature monitoring during transient states, e.g. overload.

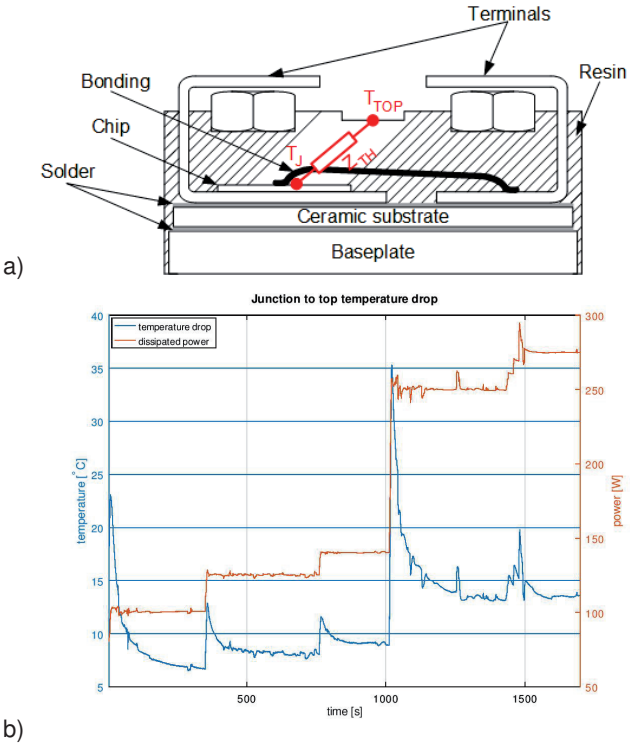

Fig. 3. Cross-section of power semiconductor device in SOT-227B housing a), difference between T_{TOP} and T_J for various levels of power losses b).

TSEP-based junction temperature measurement is the last of the methods listed in Tab. 1. This approach relies on the idea that the temperature drift of power semiconductor devices can be used for its junction temperature. The main disadvantages of TSEP-based methods are the complexity of the measurement procedure, low gain (especially in the case of SiC devices) and rather limited applicability, as not all TSEPs can be reliably measured in a real-life power converter without significant interference in its design. Nevertheless, this approach was found to be the most suitable

for developing the junction temperature measurement routine discussed in the first section, as:

1. This approach offers best accuracy among other indirect junction measurement techniques.
2. This approach allows to monitor junction temperature rise during transient states.

TSEPs for SiC power MOSFETs are further discussed in the next section.

None of the methods discussed above allow for measurement of temperature dispersion across the semiconductor chip, and such techniques are beyond the scope of the research presented.

Thermosensitive Electrical Parameters for SiC MOSFETs

Typical TSEPs can be divided into two groups: dynamic and static [17]. Examples of the first group for SiC MOSFETs include Threshold Voltage (V_{TH}), Gate Voltage Plateau (V_{GP}), Turn-on/Turn-off delay ($t_{d(on)}/t_{d(off)}$) and Turn-on transient (di/dt), while static parameters are e.g. On-state Channel Resistance ($R_{DS_{ON}}$), Breakdown Voltage ($V_{DS_{BR}}$), Body Diode Forward Voltage Drop (V_{FWD}) and Internal Gate Resistance ($R_{G_{INT}}$).

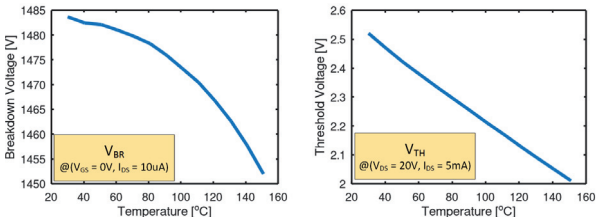

Fig. 4. Characterization of SiC power MOSFET breakdown voltage ($V_{DS_{BR}}$) and threshold voltage (V_{TH}) as TSEPs

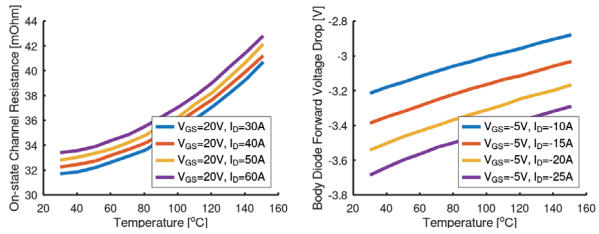

Fig. 5. Characterization of SiC power MOSFET on-state channel resistance ($R_{DS_{ON}}$) as TSEP and body diode forward voltage drop (V_{FWD}) as TSEPs

Four different TSEPs were characterized with $B1505A$ curve tracer for SiC MOSFET - $V_{DS_{BR}}$, V_{TH}, $R_{DS_{ON}}$ and V_{FWD}. Test results are given in Tab. 2 and are depicted in Figs. 4, 5, and 6. It is clear that:

1. $V_{DS_{BR}}$ and V_{TH} have negative temperature coefficient, while $R_{DS_{ON}}$ and V_{FWD} have positive.
2. $V_{DS_{BR}}$ and $R_{DS_{ON}}$ have poor linearity, which has to be taken into consideration during junction temperature estimation.
3. V_{TH} and V_{FWD} have good linearity, but rather low gain, which makes junction temperature estimation prone to error, as measuring small signals is challenging, especially in noisy environment as power converter.
4. Another drawback of V_{FWD} is fact, that high negative voltage has to be applied to the gate, to fully close the channel. Thus, current is in fact shared between $P-N$ junction and channel. V_{GS} required to fully close the channel is beyond safe operating area recommended by manufacturer, and thus it might influence reliability of tested device.
5. V_{FWD} and $R_{DS_{ON}}$ measurements are susceptible to V_{GS} amplitude applied to the tested device, which has to be taken into consideration. V_{GS} during thermal characterization has to be exactly the same as during junction temperature measurement.
6. V_{FWD} and $R_{DS_{ON}}$ measurements are susceptible to I_{DS} current flowing through the device, which has to be taken into consideration. I_{DS} during thermal characterization has to be exactly the same as during junction temperature measurement.
7. $R_{DS_{ON}}$ as TSEP has extremely small gain and is not linear. Thus, junction temperature measurement will be especially prone to error, due to measurement accuracy and small amplitude of measured signal (e.g. for probing current $\sim 1\ [A]$, measured voltage drop will be $\sim 30\ [mV]$).
8. $R_{DS_{ON}}$ and V_{FWD} can be also affected by Bias Temperature Instability, and therefore it has to be taken into consideration [18, 9] for accurate T_J measurement.

Table 2. Overview of Thermosensitive Electrical Parameters for SiC MOSFET

TSEP	Gain	Coefficient of Determination
V_{TH}	$-4.18\ [mV/°C]$	0.999233
$V_{DS_{BR}}$	$-0.2505\ [V/°C]$	0.912723
V_{FWD}	$3.059\ [mV/°C]$	0.99725
$R_{DS_{ON}}$	$0.03841\ [m\Omega/°C]$	0.948761

Beside the properties of TSEP itself, which might limit its applicability, TSEP also has to be measured in a real-life power converter without any interference in its design in order to be useful. As presented in [6, 19, 20], this disqualifies all dynamic TSEPs and $R_{G_{INT}}$, , as those parameters require a dedicated electronic circuit to be incorporated into the MOSFETs driver. The same is true with $V_{DS_{BR}}$, as such a measurement would require the power semiconductor device to be disconnected from the rest or the power converter components to avoid damaging them. This leaves only two remaining TSEPs - $R_{DS_{ON}}$ and V_{FWD} for further discussion.

Simplified diagrams of measurement circuits for those TSEPs are presented in Figs. 7a)-c). Clearly, those TSEPs do not require significant changes in either the driver circuit or switching loop. Closer analysis of these figures indicates that as long as an external probing current source is used, the measurement routine is equally complex for both V_{FWD} and $R_{DS_{ON}}$. However, in the case of $R_{DS_{ON}}$ it is possible to record voltage drop across the tested device when it is conducting working current, which is not the case for V_{FWD}. In general, such approach is discouraged [21] as it brings several concerns, such as:

- self-heating of tested device, caused by excessive conduction losses due to high current flowing through the device,
- not negligible, in comparison to measured $R_{DS_{ON}}$, resistance of terminals and interconnections within tested device,
- self-heating terminals, and interconnections within tested device,

nevertheless it can be implemented. On the other hand, when measuring with an additional probing source, the capacitance shown in Fig. 7c) has to be completely discharged before each measurement. This introduces a delay in measurement, during which the power semiconductor device cools down. Therefore, the measured value is not the actual junction temperature during operation of the power semiconductor device (e.g. in step-up configuration), but something

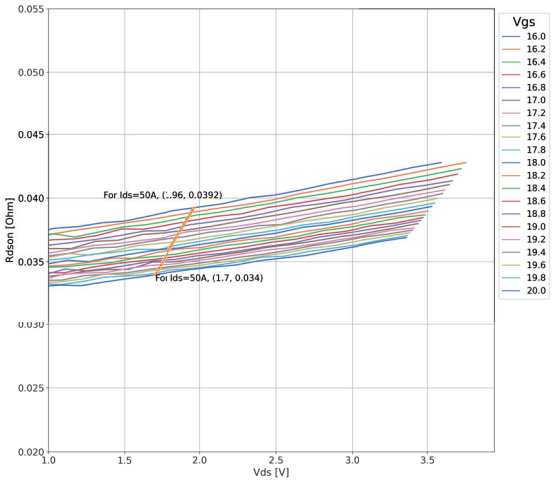

a)

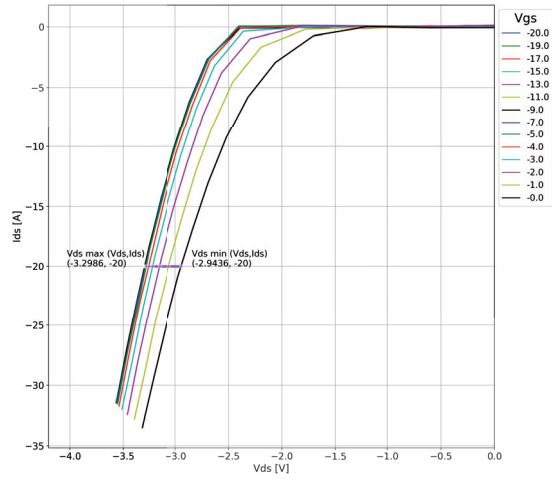

b)

Fig. 6. Dependency of $R_{DS_{ON}}$ on V_{GS} a), dependency of V_{FWD} on V_{GS} b). There is $5.2\ m\Omega$ difference in $R_{DS_{ON}}$ measured for $V_{GS} = 16\ [V]$ and $V_{GS} = 20\ [V]$.

lower, depending on the device's thermal impedance. As depicted in Fig. 8, this is a significant flaw which has to be taken into consideration.

Based on the analysis presented, it was concluded that $R_{DS_{ON}}$ is the most suitable TSEP for developing a test routine for SiC MOSFET junction temperature measurement. Next, a measurement circuit equivalent to that presented in Fig. 7c) is simple enough to be easily replicated without significant changes in the tested power converter (e.g. with voltage and current probes), and allows the measured signal (voltage drop across SiC MOSFET) to be increased, which also benefits the repeatability and accuracy of the measurement routine.

Based on the presented discussion, TSEP-based junction temperature measurement, with $R_{DS_{ON}}$ as a thermal indicator, was found to be the most suitable for a standard laboratory routine. In order to evaluate measurement accuracy, and whether there is any significant difference in results between the circuits presented in Figs. 7b)-c), further research was required.

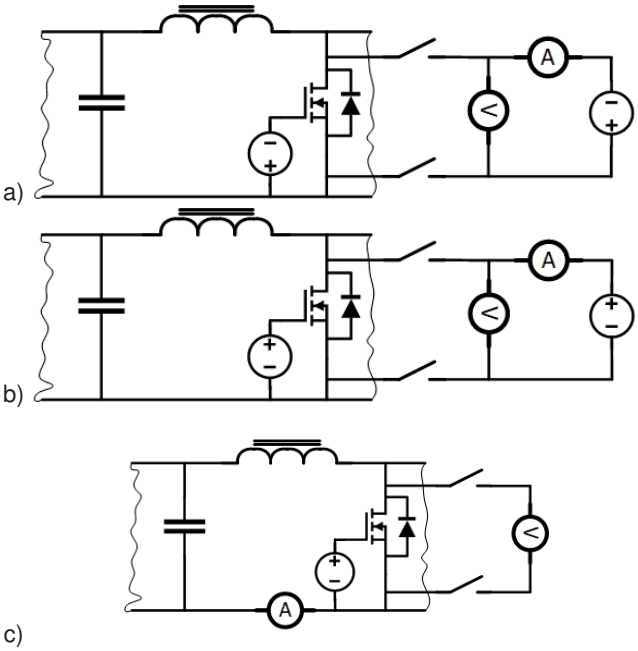

Fig. 7. Equivalent circuit for V_{FWD} measurement a), $R_{DS_{ON}}$ measurement with external probing source b), $R_{DS_{ON}}$ measurement without external probing source c) for SiC MOSFET in some power converter.

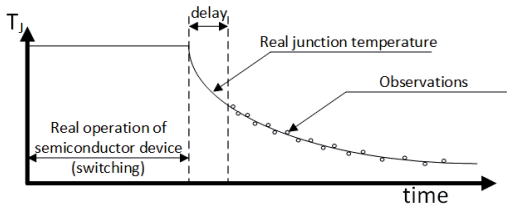

Fig. 8. Graphical representation of real junction temperature and observations for T_J estimation based on V_{FWD} and $R_{DS_{ON}}$ measurement performed with Fig. 7a)-b) circuit.

Junction temperature measurement routine

Test routine investigated in this paper is as follows:

1. Thermal characterization of chosen SiC MOSFETs was performed. During this step:
   (a) SiC MOSFETs were driven with the same driver circuit as in a real application, to mitigate issues caused by $R_{DS_{ON}}(V_{GS})$ dependency.
   (b) Thermal characterization was done for two levels of drain-source current (I_{DS}), equivalent to probing current and working current, to mitigate issues caused by $R_{DS_{ON}}(I_{DS})$ dependency.
2. The device was mounted into Active Power Cycling test bench [22] to model "real-life operating conditions". There, conduction losses were used to cause excessive heating, leading to increase of T_J.
3. T_J was measured at the end of heating pulse. Duration of heating pulse was $60\ s$, and it was optimized to ensure equilibrium.
4. In the case of method 7b):
   (a) In the last moment of the heating pulse V_{GS} was increased to nominal value for $R_{DS_{ON}}$ measurement.
   (b) Cooling curve was recorded. Measurement delay, caused by discharge of capacitances in the circuit, was verified before the test. This value was later used for extrapolation of cooling curve.
   (c) $U8001A$ laboratory power supply was used to force probing current through tested device. Prob-

ing current and voltage drop across the device were measured with $DMM6500$ digital multimeters in "data-logger" mode. Additional digital signal was used to ensure synchronization of measuring equipment.

(d) Measurements (V_{DS}, I_{DS}) were saved in CSV file, and used to calculate $R_{DS_{ON}}$.

5. In the case of method 7c):
   (a) In the last 2 $[s]$ of heating pulse V_{GS} was increased to nominal value for $R_{DS_{ON}}$ measurement.
   (b) In the last 2 $[s]$ of heating pulse, drain-source voltage (V_{DS}) and current (I_{DS}) were measured with $TCP305A$ current probe and $P2220$ voltage probe, and recorded with $DPO3014$ oscilloscope.
   (c) Same measurement routine was repeated with $DMM6500$ multimeter and $TCP305A$ current probe. Multimeter operated in "data-logger" mode.
   (d) In the case of oscilloscope-based measurement, V_{DS} and I_{DS} waveforms were averaged for 100 $[\mu s]$ windows. These averaged values were used to calculate $R_{DS_{ON}}$.
   (e) In the case of multimeter-based measurement, V_{DS} was recorded in "data-logger" mode. I_{DS} was measured with other multimeter. $R_{DS_{ON}}$ was calculated afterwards with V_{DS} and I_{DS} readings.

As stated above, to heat up SiC MOSFET, it was put into linear region to increase conduction losses. Thus, when V_{GS} was increased to nominal value in the last 2 $[s]$ of heating pulse, conduction losses dropped back to a minimimum, which essentially causes cooling of the device. Therefore, each method - 7b), 7c) with oscilloscope and digital multimeter - is used to record a "cooling curve", but in different ways and with different measurement delay.

Last step of measurement routine was the same for all cases: a Particle Swarm Optimization algorithm was used to fit mathematical function given in Eq. 2, to measured values of $R_{DS_{ON}}$[23].

$$R_{DS_{ON}}(t) = p_1 + p_2 \cdot e^{\frac{t}{p_3}} + p_4 \cdot e^{\frac{t}{p_5}} \tag{2}$$

Where, $R_{DS_{ON}}(t)$ is function of on-state channel resistance during cooling of SiC MOSFET, p_n are model parameters, t is time given in $[ms]$. Next, the fitted mathematical function was used to interpolate measurements, and extrapolate data to t_0 - the moment when V_{GS} was increased to nominal value. Finally, T_J was calculated based on $R_{DS_{ON}}$ and conversion function, which is further described in the next section.

Test results

To evaluate the measurement methods discussed above, they were used to measure the junction temperature of an $FF11MR12W1M1B11$ SiC module. This particular module was chosen as it is equipped with an NTC temperature sensor, which was used as a reference measurement. In the first step, the conversion function allowing calculation of T_J based on $R_{DS_{ON}}$ had to be identified. For this purpose, module was heated up from $25°C$ to $150°C$ with $10°C$ step, and $R_{DS_{ON}}$ was measured each time for exactly the same driving conditions as in the following test. Next, an approximation function, given in Eq. 3, where T_J is junction temperature, p_n are model parameters and $R_{DS_{ON}}$ is on-state channel resistance, was fitted to those data.

$$T_J = p_1 \cdot ln(R_{DS_{ON}}) - p_2 \tag{3}$$

Next, the junction temperature of $FF11MR12W1M1B11$ SiC module was measured according to the description of test routines given in previous section, starting from routine 7c) with an oscilloscope. As depicted in Fig. 9, the change of V_{GS} to nominal value caused a transient state, which introduced measurement delay of ~ 468 $[\mu s]$. After that, measurements of V_{DS} and I_{DS} were recorded and averaged in 100 $[\mu s]$ time windows. Next, the other test routines were performed.

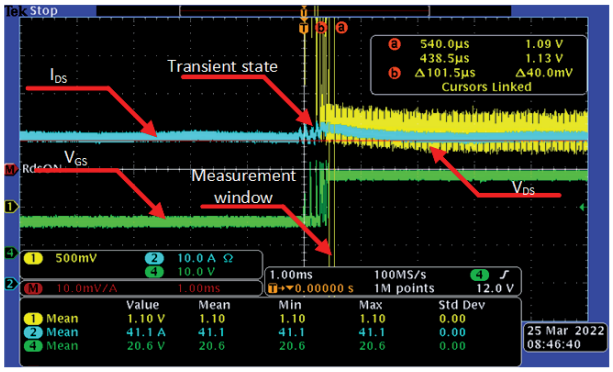

Fig. 9. $R_{DS_{ON}}$ measurement with oscilloscope. V_{DS} and I_{DS} were recorded and averaged in 100 $[\mu s]$ time windows.

After laboratory tests, a Particle Swarm Optimization (PSO) algorithm was used to fit proper approximation function (see Eq. 2) to recorded data. As depicted in Fig. 10, in each case the PSO algorithm ensured good fit of proposed model to data. Closer analysis on relative error distribution, shows that fitting is especially good for first part of recorded data, for the beginning of the cooling curve. This suggests that the selected approximation function properly describes the changes in $R_{DS_{ON}}$ during cooling of the SiC module, and it can therefore be used for extrapolation on $R_{DS_{ON}}(t)$ for t smaller than measurement delay caused by transient state, discharging capacitance in the test bench and other factors.

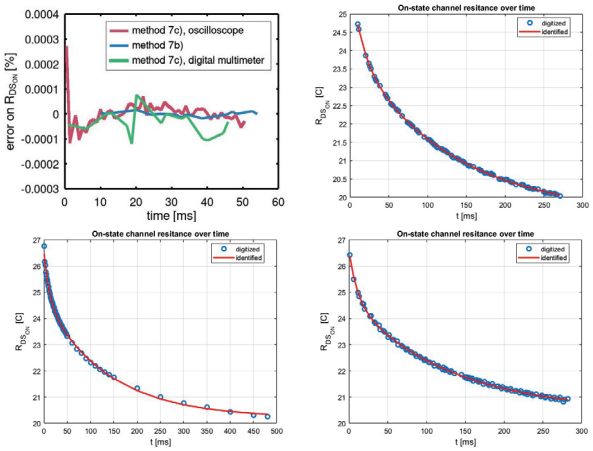

Fig. 10. Curve fitting to $R_{DS_{ON}}$ measurements recorded with method 7b) on the top right, and those recorded with method 7c) on the bottom (oscilloscope measurement - left, digital multimeter - right). Relative error distribution for first 50 $[ms]$ of the record on the top left.

Test results depicted in Fig. 11 shows that all the measurements follows the same cooling curve in the first 30 $[ms]$. Afterwards, cooling curves diverge due to conduction losses dissipated in the devices. Fitted curves meets at $\sim 117.5°C$ ($117.53°C$, $117.54°C$, $117.7°C$ for values extrapolated based on the test routine 7b), 7c) with an oscilloscope and 7c) with a digital multimeter respectively). Although first sample recorded with the oscilloscope indicates a

higher junction temperature ($119.09°C$), this might be related to measurement accuracy. A comparison of actual measurements, fitted values and worst-case measurement accuracy is depicted in Fig. 12. Next, a closer analysis of this Figure indicates that test routine 7b) offers the lowest accuracy, although digital multimeters used in the test have far better accuracy than the setup consisting of digital oscilloscope, and probes. This phenomenon was caused by the weak amplitude of signals measured (I_{DS}, V_{DS}) in test routine 7b). Also, the best accuracy was offered by test routine 7c) where V_{DS} was recorded with high-class digital multimeter, and I_{DS} was measured with a current probe. Finally, the test results presented above corresponds to reference T_J measurement, based on the reading of embedded NTC sensor, which indicated $T_J \sim 115°C \pm 10°C$.

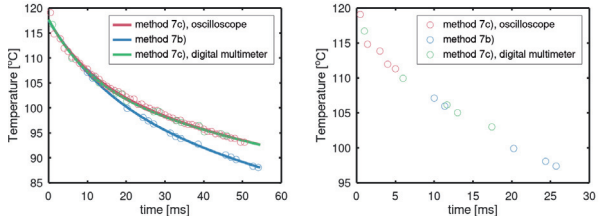

Fig. 11. Junction temperature measurements (circle), fitted values (solid line). Magnification on the first 30 $[ms]$ of cooling curve on the right side.

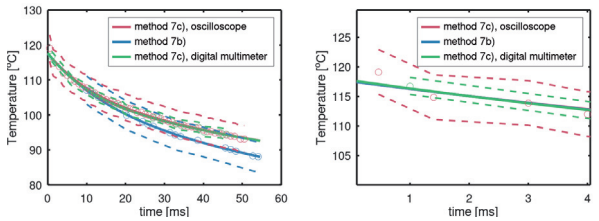

Fig. 12. Junction temperature measurements (circle), fitted values (solid line) and worst-case measurement accuracy (dashed line). Magnification on the first 4 $[ms]$ of cooling curve on the right side.

Conclusion

The presented test results show that on-state channel resistance can be successfully utilized in the role of TSEP for junction temperature measurement of SiC MOSFETs in real-life operating conditions. Cross-comparison of different measurement routines shows that $R_{DS_{ON}}$ measurement performed with an oscilloscope and a set of voltage and current probes offers satisfactory accuracy, enabling the shortest measurement delay (< 500 $[\mu s]$). Although performing the same test routine with a high-class digital multimeter ensures greater accuracy, there is no significant difference in results for those two methods.

Also, when cooling curves were used to fit the mathematical function and extrapolate T_J at the very end of a heating pulse, the differences in extrapolated values were even smaller ($< 0.3°C$). The difference between the extrapolated value and actual measurement was $< 2°C$, which indicates that test routine 7c) with an oscilloscope is suitable for purposes of daily operation of the R&D department.

Finally, the proposed test routine offers similar accuracy to junction temperature measurement based on an embedded temperature sensor, while resolving the main drawbacks of this method: 1) dependency of T_J estimation on environmental factors, 2) applicability limited only to power semiconductor devices equipped with a built-in temperature sensor.

***Authors**: Ph.D. Sebastian Bąba, M.Sc. Grzegorz Palesa, M.Sc. Jarosław Wiśniewski, B.Sc. Filip Manka Research and Development Department TRUMPF Huettinger Sp. z o. o. ul. Marecka 47 05-220 Zielonka, Poland email: sebastian.baba@trumpf.com*

REFERENCES

[1] Ying Zhang, Luhong Xie, Yuxing Yan, Yushan Zhao, Yongzhang Huang, and Erping Deng. Investigation on vsd(t) and vds,on(t) methods for cascode gan device junction temperature measurement. In *2023 IEEE 6th International Electrical and Energy Conference (CIEEC)*, pages 3095–3098, 2023.

[2] E. R. Motto and J. F. Donlon. Igbt module with user accessible on-chip current and temperature sensors. In *2012 Twenty-Seventh Annual IEEE Applied Power Electronics Conference and Exposition (APEC)*, pages 176–181, Feb 2012.

[3] Konrad Markowski, Juliusz Bojarczuk, Piotr Araszkiewicz, Jakub Ciftci, Adam Ignaciuk, and Michał Gąska. High temperature measurement with low cost, vcsel-based, interrogation system using femtosecond bragg gratings. *Sensors*, 22(24), 2022.

[4] Konrad Markowski, Juliusz Bojarczuk, Piotr Araszkiewicz, Robert Cybulski, Michal Gaska, and Arkadiusz Golaszewski. Analysis of the performance of wdm-cdm bragg grating interrogation system with high-contrast grating vcsel. *Journal of Lightwave Technology*, 41(9):2892–2903, 2023.

[5] Haoze Luo, Junjie Mao, Chengmin Li, Francesco Iannuzzo, Wuhua Li, and Xiangning He. Online junction temperature and current simultaneous extraction for sic mosfets with electroluminescence effect. *IEEE Transactions on Power Electronics*, 37(1):21–25, 2022.

[6] A. Griffo, J. Wang, K. Colombage, and T. Kamel. Real-time measurement of temperature sensitive electrical parameters in sic power mosfets. *IEEE Transactions on Industrial Electronics*, 65(3):2663–2671, March 2018.

[7] Dan Zheng, Yuhui Kang, Han Cao, Xiaoguang Chai, Tao Fan, and Puqi Ning. Monitoring of sic mosfet junction temperature with on-state voltage at high currents. *Chinese Journal of Electrical Engineering*, 6(3):1–7, 2020.

[8] Fumiki Kato, Shinji Sato, Kenichi Koui, Hidekazu Tanisawa, Hiroshi Hozoji, and Hiroshi Yamaguchi. Study of gate bias voltage for preventing threshold shift of sic–mosfet body diode during transient temperature measurements. In *2019 International Conference on Electronics Packaging (ICEP)*, pages 88–91, 2019.

[9] Jose Ortiz Gonzalez and Olayiwola Alatise. Bias temperature instability and junction temperature measurement using electrical parameters in sic power mosfets. *IEEE Transactions on Industry Applications*, 57(2):1664–1676, 2021.

[10] B. Shi, S. Feng, L. Shi, D. Shi, Y. Zhang, and H. Zhu. Junction temperature measurement method for power mosfets using turn-on delay of impulse signal. *IEEE Transactions on Power Electronics*, 33(6):5274–5282, June 2018.

[11] H. Kuhn and A. Mertens. On-line junction temperature measurement of igbts based on temperature sensitive electrical parameters. In *2009 13th European Conference on Power Electronics and Applications*, pages 1–10, Sep. 2009.

[12] N. Baker, S. Munk-Nielsen, F. Iannuzzo, and M. Liserre. Online junction temperature measurement using peak gate current. In *2015 IEEE Applied Power Electronics Conference and Exposition (APEC)*, pages 1270–1275, March 2015.

[13] T. Hunger and R. Bayerer. Extended reliability of substrate solder joints in power modules. In *2009 13th European Conference on Power Electronics and Applications*, pages 1–8, Sep. 2009.

[14] Sebastian Baba, Marek Jasinski, and Marcin Zelechowski. Temperature measurement of rf power amplifier. In *2020 19th International Power Electronics and Motion Control Conference*, pages 1–1, 2021.

[15] T. Krone, L. Dang Hung, M. Jung, and A. Mertens. On-line semiconductor switching loss measurement system for an advanced condition monitoring concept. In *2016 18th European Conference on Power Electronics and Applications (EPE'16 ECCE Europe)*, pages 1–10, Sep. 2016.

[16] Julian Weimer, Dominik Koch, and Ingmar Kallfass. Accuracy study of calorimetric switching loss energy measurements for wide bandgap power transistors. In *2021 23rd European Conference on Power Electronics and Applications (EPE'21 ECCE Europe)*, pages P.1–P.9, 2021.

[17] L. Li, P. Ning, D. Zhang, and X. Wen. An exploration of thermo-sensitive electrical parameters to estimate the junction temperature of silicon carbide mosfet. In *2017 IEEE Transportation Electrification Conference and Expo, Asia-Pacific (ITEC Asia-Pacific)*, pages 1–5, Aug 2017.

[18] J. Ortiz Gonzalez and O. Alatise. Challenges of junction temperature sensing in sic power mosfets. In *2019 10th International Conference on Power Electronics and ECCE Asia (ICPE 2019 - ECCE Asia)*, pages 891–898, 2019.

[19] J. Kuprat, C. H. Van der Broeck, M. Andresen, S. Kalker, R. W. De Doncker, and M. Liserre. Research on active thermal control: Actual status and future trends special issue commemorating 40 years of wempec, 2021. *IEEE Journal of Emerging and Selected Topics in Power Electronics*, pages 1–1, 2021.

[20] H. Niu and R. D. Lorenz. Real-time junction temperature sensing for silicon carbide mosfet with different gate drive topologies and different operating conditions. *IEEE Transactions on Power Electronics*, 33(4):3424–3440, April 2018.

[21] Thomas Harder. Qualification of power modules for use in power electronics converter units in motor vehicles, May 2021.

[22] S. Baba, A. Gieraltowski, M. T. Jasinski, F. Blaabjerg, A. S. Bahman, and M. Zelechowski. Active power cycling test bench for sic power mosfets - principles, design and implementation. *IEEE Transactions on Power Electronics*, pages 1–1, 2020.

[23] S. Baba, M. Zelechowski, and M. Jasinski. Estimation of thermal network models parameters based on particle swarm optimization algorithm. In *2019 IEEE 13th International Conference on Compatibility, Power Electronics and Power Engineering (CPE-POWERENG)*, pages 1–6, 2019.